DOI: 10.1002/chem.200600808

Hydrogen-Bond Interactions of Nicotine and Acetylcholine Salts: A Combined Crystallographic, Spectroscopic, Thermodynamic and Theoretical Study

Virginie Arnaud,[a] Michel Berthelot,[a] Michel Evain,[b] Jérôme Graton,[a] and Jean-Yves Le Questel*[a]

Abstract: The hydrogen-bond (HB) interactions of the monocharged active forms of nicotine and acetylcholine (ACh) have been compared theoretically by using density functional theory (DFT) calculations and experimentally on the basis of crystallographic observations and the measurement of equilibrium constants in solution. The 2,4,6-trinitrophenolate (picrate) counterion was used to determine the experimental HB basicity of the cations despite its potential multisite HB acceptor properties. The preferred HB interaction site of the ammonium picrate salts was determined from a survey of crystallographic data found in the Cambridge Structural Database (CSD) and is supported by theoretical calculations. Two distinct classes of ammonium groups were characterised depending on the absence (quaternary ammonium) or presence (tertiary, secondary and primary ammoniums) of an $N^+H\cdots O$ hydrogen bond linking the two ions. The crystal structure of nicotinium picrate was determined and compared with that of ACh. This analysis revealed the peculiar behaviour of the ammonium moiety of nicotinic acetylcholine receptor (nAChR) ligands towards the picrate anion. Dedicated methods have been developed to separate the individual contributions of the anion and cation accepting sites to the overall HB basicity of the ion pairs measured in solution. The HB basicities of the picrate anions associated with the two different ammonium classes were determined in dichloromethane solution by using several model ion pairs with non-basic ammonium cations. The experimental and theoretical studies performed on the nicotine and ACh cations consistently show the significant HB ability of the acceptor site of nAChR agonists in their charged form. Both the greater HB basicity of the pyridinic nitrogen over the carbonyl oxygen and the greater HB acidity of the N^+H unit relative to N^+CH could contribute to the higher affinity for nAChRs of nicotine-like ligands relative to ACh-like ligands.

Keywords: density functional calculations · hydrogen bonds · IR spectroscopy · molecular recognition · nAChR agonists · X-ray diffraction

Introduction

Nicotinic acetylcholine receptors (nAChRs) are ligand-gated ion channels that mediate neurotransmission at the neuromuscular junction, both in the peripheral nervous system and at numerous sites in the central nervous system (CNS). During the last decade, nAChRs have appeared as valid targets for treatments against a wide variety of diseases such as cognitive and attention deficits, Parkinson's and Alzheimer's diseases and anxiety and pain management.[1,2] The functional importance of CNS nAChRs and their involvement in numerous pathologies have led to a great number of investigations aimed at their structural characterisation.[3,4] However, as for most membrane proteins, structural information about nAChRs is sparse because they are difficult to purify. The best experimental structure derived for nAChRs con-

[a] Dr. V. Arnaud, Prof. Dr. M. Berthelot, Dr. J. Graton, Prof. Dr. J.-Y. Le Questel
Laboratoire de Spectrochimie et Modélisation
EA 1149, FR CNRS 2465, Université de Nantes
Nantes Atlantique Universités
Faculté des Sciences et des Techniques de Nantes
2, rue de la Houssinière, BP 92208, 44322 Nantes Cedex 3 (France)
Fax : (+33) 251-125-567
E-mail: Jean-Yves.Le-Questel@univ-nantes.fr

[b] Prof. Dr. M. Evain
Laboratoire de Chimie du Solide
(Institut Jean Rouxel, CNRS UMR 6502)
Université de Nantes, Nantes Atlantique Universités
Faculté des Sciences et des Techniques de Nantes
2, rue de la Houssinière, BP 92208, 44322 Nantes Cedex 3 (France)

sists of 4.0 Å data obtained from cryoelectron microscopy,[5] a resolution that does not allow structure-based design approaches.

Recently, the crystal structure of an acetylcholine binding protein (AChBP) was established as the model for the extracellular domain of nAChRs, which contains the ligand-binding domain (LBD).[6] Furthermore, the resolution of its complexes with nicotine (**1**) and carbamylcholine,[7] both agonists of ACh (**2**), have validated the pharmacophore

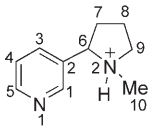

1

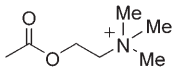

2

models of Beers and Reich[8] that have been the subject of extensive study since the 1970s.[9–11] The two key elements of the nAChR pharmacophore models, a quaternised nitrogen atom and a hydrogen-bond (HB) acceptor site, are directly involved in non-covalent interactions with residues of the receptor. However, a detailed analysis of these interactions and of their relative importance in the docking process into the nAChRs requires high-resolution X-ray data. Dougherty and co-workers[12] recently showed how a physical chemistry approach can provide high-precision insights into nAChR–agonist interactions. In the same vein, in a comprehensive investigation based on a wide variety of computational methods, Huang et al.[13] identified the dominant factors differentiating the binding strength of agonists in several forms. Among these factors, hydrogen bonding was recognised as playing a key role, both at the HB acceptor site of the agonists and at the ammonium site. Despite this importance, investigations devoted to the study of nAChR HB properties are scarce. The neutral form of nicotine, nornicotine, and models of these compounds have been the subject of detailed experimental and theoretical studies,[14] whereas the agonists interact with nAChRs in their charged form. A recent computational investigation of protonated nicotine has thrown light on the influence of this charge, and of its partial or full neutralisation, on the HB accepting properties of the pyridine sp^2 nitrogen atom.[15] Moreover, on the basis of crystal structures and calorimetric studies, Celie et al.[7] have shown that the greater affinity of nicotine relative to carbamylcholine is partly due to the presence of an HB interaction between the protein and nicotine. We have recently confirmed by using experimental and theoretical data that the sp^2 nitrogen atom is indeed a significant HB acceptor in monoprotonated nicotine,[16] but this is, to the best of our knowledge, the only experimental study devoted to the analysis of the HB properties of ACh agonists in their active form. This quantification is clearly important for a deeper characterisation of the hydrogen-bonding interactions occurring in their docking into nAChRs and a rationalisation of their respective affinities.

In preliminary work[16] we have shown that the picrate anion (Pic^-) is the most convenient counterion because it combines several interesting and/or essential properties: 1) the salts are readily synthesised by direct neutralisation of the amine with picric acid or by precipitation of silver iodide between silver picrate and the ammonium iodide,[17] 2) the picrates of ternary and quaternary ammonium ions are generally soluble enough in low polarity solvents to enable quantitative physico-chemical measurements, 3) the asymmetrical geometry and the large size of the anion drastically reduce the association of the ion pair into polymeric species in solvents of low dielectric constants[18,19] and 4) the competing hydrogen-bond accepting strength of the anion is very weak, of the same order of magnitude as that of the perchlorate ion.[20] This work supplements our preliminary investigation of the HB properties of charged nicotine in two ways. First, we investigated the HB interactions of ammonium–picrate systems from a survey of crystallographic data found in the Cambridge Structural Database (CSD). The crystal structure of nicotinium picrate was determined allowing a direct comparison with the known structure of ACh picrate. Then, we carried out experimental measurements and theoretical (B3LYP/6-31+G** level) estimations of the HB basicity of the sp^2 nitrogen atom of different monoprotonated nicotinoids and of the carbonyl oxygen atom of ACh and its models.

Altogether, the different analyses carried out in the solid state, in solution and in the gas phase provide a coherent set of data allowing, for the first time, a detailed comparison of the two charged ligands and revealing important information about the hydrogen-bonding interactions of both pharmacophore elements of ACh and nicotine.

Results and Discussion

CSD searches

Preferred site of interaction of the picrate anion: The picrate anion contains several non-equivalent organic functionalities that are able to interact with a positively charged entity: the phenolate and the three nitro groups. This situation is complicated even more by the fact that the nitro groups themselves present several interaction motifs (Scheme 1), for example, with regard to hydrogen bonding.[21] Allen et al. have shown in their study of the HB properties of nitro oxygen atoms[21] that of the three possibilities presented in

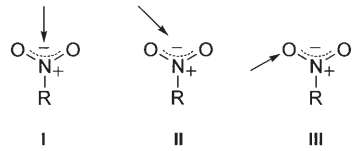

Scheme 1. Directionality of the HB contacts with the nitro group.

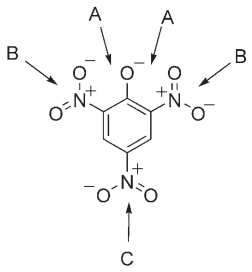

Scheme 2. Directionality of the HB contacts with the picrate anion.

Scheme 1, the two bidentate motifs I and II are clearly preferred over the monodentate motif III. On this basis, five directions of approach of the positively charged group, corresponding to three types of association, A, B and C, have been considered (Scheme 2).

In addition to these potential interactions of the different oxygen atoms with charged groups and/or HB donors, π–π interactions through the picrate aromatic ring also contribute to molecular recognition processes.[22] For all these reasons, picric acid appears a versatile agent particularly well suited to probing the competition between various intermolecular forces in crystal engineering.[23] To determine the favoured motif of HB association (A, B or C), we have listed in Table 1 their distribution among the five ammonium series, in addition to the total number of interactions. An intermolecular contact was defined as in the IsoStar library,[24] that is, as any contact shorter than $V+0.5$ Å, where V is the sum of the Bondi van der Waals radii. In the present case, this criterion corresponds to a distance of 3.6 Å.[25]

Table 1. Distribution of the ammonium–picrate contacts observed in the CSD according to the ammonium and association types.

	NH_4^+	NH_3Z^+	$NH_2Z_2^+$	NHZ_3^+	NZ_4^+
N_T[a]	14 (5)	144 (43)	77 (28)	60 (41)	8 (7)
motif A[b]					
N_A (N_A/N_T [%])[c]	8 (57)	75 (52)	43 (56)	48 (83)	8 (100)
short contacts [%][d]	100	99	93	100	0
motif B[b]					
N_B (N_B/N_T [%])[c]	4 (29)	22 (15)	7 (9)	1 (2)	0 (0)
short contacts [%][d]	100	68	57	0	–
motif C[b]					
N_C (N_C/N_T [%])[c]	2 (14)	47 (33)	27 (35)	11 (15)	0 (0)
short contacts [%][d]	100	33	15	9	–

[a] Total number of interactions with the number of refcodes given in parentheses. [b] The A, B and C notation is defined in Scheme 2. [c] The number of contacts shorter than 3.6 Å with the corresponding percentage in the ammonium series is given in parentheses. [d] Percentage of contacts shorter than the sum of the van der Waals radii ($V=3.10$ Å) among the N_i contacts.

Table 1 shows that the highest number of contacts is systematically observed for mode A, which corresponds to interactions between the ammonium and the phenolate group. Then, with the exception of the NH_4^+ series, mode C appears to be preferred significantly over mode B. Moreover, the limitation of the distance criterion to $V=3.10$ Å drastically reduces the percentage of short contacts in motifs B and C as nitrogen alkylation increases, while motif A remains unchanged. These observations confirm that the main interactions involve the phenolate group. Contacts observed at the *ortho*- and *para*-nitro groups can thus only be defined as secondary interactions, generally present when the ammonium group is already engaged with the phenolate moiety of a first picrate anion. Another interesting observation that can be made from the data in Table 1 is the peculiar behaviour of the quaternary ammonium–picrate substructure, which presents a unique interaction motif A with a very low number of contacts and a lack of any short contact. These features reflect the greater steric crowding around the ammonium nitrogen atom, preventing the approach of the picrate oxygen atoms.

Geometry of ammonium–picrate interactions: Geometrical analyses of the $N^+\cdots O^-$ interactions were carried out by using the parameters indicated in Figure 1, which represents an example of the interaction motifs. The distances between the positive nitrogen atom and the phenolic or nitro oxygen atoms are noted as d_1 and d_2, respectively. The α_1 and α_2 valence angles indicate the interaction directionality, whilst the dihedral angles φ_1 and φ_2 describe, respectively, the position of the ammonium nitrogen atom and the rotation of the adjacent NO_2 group relative to the plane of the picrate anion ring.

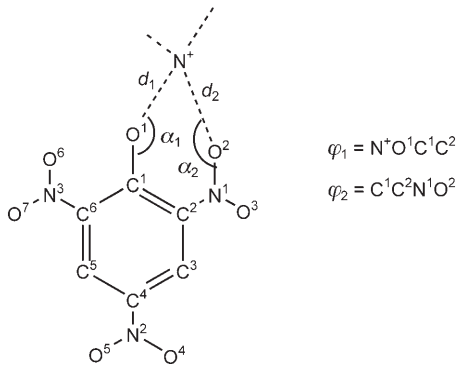

Figure 1. Numbering and geometrical parameters of the picrate anions.

Because the preferred picrate site of interaction corresponds without ambiguity to the A motif, we only analysed the geometric parameters of the ammonium–picrate contacts in this configuration. The distances d and the angles α are presented in Table 2 as a function of ammonium type.

Table 2. Geometries[a] observed in the CSD for ammonium–picrate contacts in motif A.

Ammonium	d_1 [Å]	d_2 [Å]	α_1 [°]	α_2 [°]
NH_4^+	2.88(2)	3.00(5)	125(5)	131(5)
NH_3Z^+	2.86(2)	3.03(2)	131(2)	132(2)
$NH_2Z_2^+$	2.82(2)	3.12(3)	135(2)	140(2)
NHZ_3^+	2.76(3)	3.18(3)	146(1)	135(2)
NZ_4^+	3.49(2)	4.32(5)	166(4)	135(3)

[a] The geometric parameters are defined in Figure 1. The standard errors referring to the last significant digit are indicated in parentheses.

The φ_1 and φ_2 dihedral histograms of the primary ammonium contacts NH_3Z^+, which present the greatest number of interactions, are shown in Figure 2.

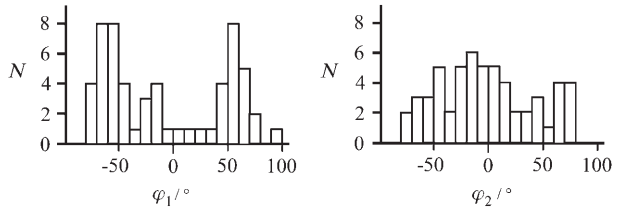

Figure 2. Histograms of the φ_1 and φ_2 dihedral angles for primary ammonium–picrate contacts.

It appears from the data in the last column of Table 2 that the α_2 valence angle does not differ significantly between the different types of ammonium groups. The average value of around 135° indicates a cooperative participation of a nitro oxygen lone pair in the overall interaction. Conversely, the α_1 valence angle does vary significantly, from 125° for NH_4^+–picrate contacts to 166° for quaternary ammonium ones. This evolution reflects the progressive crowding of the nitrogen atom, which induces more linear interactions with the phenolate oxygen in the case of quaternary ammonium picrates.

As seen in Figure 2, the two dihedral angles φ_1 and φ_2 also behave differently. On the one hand, the values of φ_1, with a predilection for values of $\pm 60°$, reveal that the ammonium nitrogen atom is not in the plane of the picrate anion. On the other hand, the very large range of φ_2 values indicates that the *ortho*-nitro group freely twists its plane to better accommodate the cation position.

The variations in the distances d reported in Table 2 are also very informative. Direct comparison of d_1 and d_2 shows that the bonding motifs are always asymmetric, the ammonium nitrogen being closer to the phenolate oxygen atom for all types of cation. The distances d_1 and d_2 discriminate clearly between two very distinct classes of ammonium picrates. The first class, with mean values $d_1 = 2.83(5)$ and $d_2 = 3.08(8)$ Å, includes all types of ammonium cation bearing at least one N^+–H bond. A closer inspection of the structures shows that the interactions correspond to strong $(N^+)H\cdots O^-$ hydrogen bonds. The separations d_1 and d_2 between the two ions are distinctly larger for quaternary NZ_4^+ ammoniums ($d_1 = 3.49(2)$, $d_2 = 4.32(5)$ Å), which constitute the second class.

Crystal structures

Conformation of the nicotinium cation in the picrate salt: The geometrical parameters generally used to describe nicotine (**1**) derivatives are 1) the *syn* or *anti* position of the N^2-methyl substituent relative to the pyridine ring, 2) the relative position of the two rings and 3) the conformation of the pyrrolidine ring. In the crystal structure of nicotinium picrate, the methyl group carried by the N^2 nitrogen atom is in an equatorial position, that is to say, *anti* with respect to the pyridine ring. The C^1-C^2-C^6-C^7 dihedral angle of −126.8° corresponds to a roughly perpendicular orientation of the pyridine and pyrrolidine rings. These features are in agreement with previous investigations of neutral and charged forms of nicotine and appear general whatever the physical state.[26–30] Conversely, the envelope conformation of the pyrrolidine ring has been shown to depend on the state of the molecule.[30,31] In this work, the five-membered ring envelope is characterised by an out-of-plane position of the C^6 carbon atom, whereas in its neutral form the N^2 nitrogen atom occupies this position. The geometry of the nicotinium cation corresponds to the **A** conformer, the most stable in the gas phase.[29,31] There has been much debate about the optimal internitrogen $N^1\cdots N^2$ distance in the nicotinic pharmacophore for maximal binding affinity.[10] The $N^1\cdots N^2$ distance of 4.70 Å observed in nicotinium picrate is of the same order of magnitude as the value obtained for the nicotine hydroiodide salt by Barlow and Johnson[32] and is close to the 4.4 ± 0.1 Å distance observed for nicotine in the AChBP binding site.[7]

Comparison of ACh and nicotinium picrates: The HB interactions between the ammonium groups of the nicotinium and ACh cations (refcode: GEBMEF)[33] and the picrate anion are displayed in Figure 3a and 3b, respectively. Note

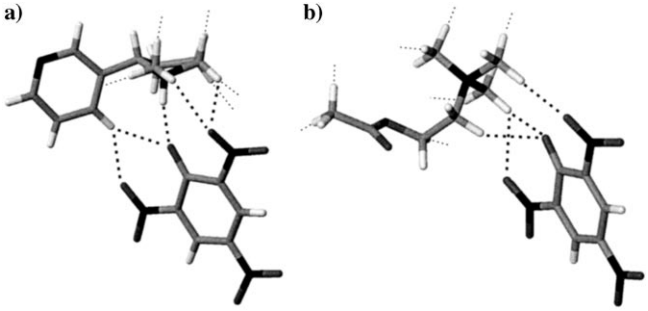

Figure 3. Crystal structures of a) nicotinium and b) ACh picrate ion pairs. The short contact network observed in the asymmetric unit is shown by the dotted lines. The contacts specific to the ion pairs are shown as bold dots.

that both crystalline structures reveal π–π stacking interactions between two Pic^- anions in GEBMEF and between the pyridyl ring and the Pic^- anion in the nicotinium picrate. We only examine here the HB interactions between the ammonium moieties and the picrate anion. The main hydrogen bond in the nicotinium picrate ion pair involves the ammonium NH^+ and the phenolate O^- groups ($d_{H^+\cdots O^-} = 1.863$ Å). The d_1 and d_2 values of 2.767 and 3.146 Å, respectively, are of the same order of magnitude as the corresponding mean values for the NHZ_3^+ ammonium cations (2.76(3) and 3.18(3) Å) presented in Table 2. This is also true for the directionalities as the α_1 and α_2 angles of 150.3 and 126.5°, respectively, compare reasonably well with the corresponding

146(1) and 135(2)° values given in Table 2. The ammonium nitrogen atom is located in the plane of the picrate anion ring, as shown by the φ_1 value (2.6°). In addition, a significant twist of the nitro group is revealed by the φ_2 value (−67.3°). This rotation allows additional short contacts with the hydrogen atoms of the methyl and methylene groups to form (Figure 3a). With its phenolate oxygen atom and its three nitro groups, the picrate anion contains many HB acceptor sites able to provide secondary interactions with the hydrogen atoms of the cation. Indeed, not less than 8 of the 15 hydrogen atoms of the nicotinium cation are engaged in 10 contacts that are less than the sum of the van der Waals radii of the hydrogen and oxygen atoms (2.65 Å).[25,34] The shortest one (1.863 Å) corresponds as expected to the $(N^+)H\cdots O^-$ interaction, this ammonium hydrogen atom also being engaged in a secondary contact with the oxygen atom of an *ortho*-nitro group. The eight remaining contacts can be divided into two groups involving six hydrogen atoms of the methylpyrrolidinium group on the one side and a pyridyl hydrogen atom on the other. In comparison, 10 of the 16 hydrogen atoms of the ACh picrate are involved in 11 short contacts with either different picrate moieties or the carbonyl group of another ACh molecule. These hydrogen atoms belong both to CH groups directly linked to the ammonium nitrogen atom and also to the acetyl group (Figure 3b). The mean distance of these 11 (C)H···O contacts (2.413 Å) is significantly shorter than the corresponding one for the nicotinium cation (six (C)H···O contacts, 2.551 Å). This suggests that the positive charge on the nitrogen atom is spread considerably more over the adjacent CH bonds in ACh than in the nicotinium cation, in which the charge is more localised on the NH group. Finally, note that such CH···O interactions are observed in the crystal structures of nicotine and carbamylcholine bound to AChBP[7] and have recently been reported by Dougherty[12] and Huang[13] and their co-workers in their molecular modelling studies devoted to their docking into nAChR models. These contacts involve nicotine and carbamylcholine CH groups and the oxygen atoms of protein residues (the carbonyl group of tryptophan and the phenolic oxygen atom of tyrosine).

Theoretical calculations

Electrostatic potentials of the naked anion and cations: Analysis of the electrostatic potentials on the picrate ion surface ($V_{s,min}$) is particularly well suited to highlighting the behaviour of its various organic functionalities. Sawada et al., through V_{min} calculations (HF/6-31G*),[35] and Troxler et al., from an analysis of partial atomic charges fitted on electrostatic potentials,[36] found that the most electron-rich site of the anion is the phenolate oxygen. These results indicate that the internal charge transfer toward the strong electron-withdrawing nitro substituents is not sufficient to completely deplete its negative charge in favour of the nitro oxygen atoms. Our calculations at the B3LYP/6-31+G** level of theory, presented in Figure 4, confirm the pre-eminence of site A in agreement with the preference observed in crystalline picrate environments (Table 1). Furthermore, the location of the minima clearly supports the favoured bidentate nature of the interaction with the nitro groups (motifs I and II of Scheme 1).

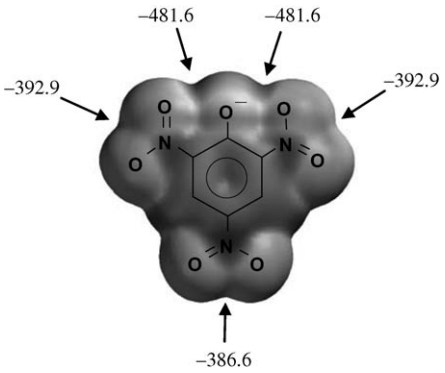

Figure 4. Electrostatic potential map of the naked picrate anion at the molecular surface (values shown are $V_{s,min}$ [kJ mol^{-1}]).

The most positive electrostatic potentials of the naked ACh cation surface appear approximately in the direction of the centres of the four triangular faces formed by the carbon atoms of the $CH_2N^+(CH_3)_3$ distorted tetrahedron. This preference of a basic centre to bind to hydrogen atoms belonging to different carbon atoms rather than to the same one has already been rationalised through theoretical calculations.[37] The electrostatic potential maximum is located on the face formed by the methylene and two methyl groups, which is opposite the acetoxy substituent. As shown in Figure 3, this is indeed the face selected by the negative oxygen atom of the picrate anion in the solid state. The NH^+ proton of the naked $NicH^+$ cation surface exhibits the maximum electrostatic potential. The $V_{s,max} = 593$ kJ mol^{-1} value is about 90 kJ mol^{-1} higher than the maximum induced by three cooperative protons of the $CH_2N^+(CH_3)_3$ group of ACh.

Electrostatic potentials of the ion pairs: The ion-pair electrostatic potentials presented in Figure 5 for different ammonium picrates are also very useful. First, the electrostatic potential minima around the two nitro groups in the *ortho* position are now always different owing to the asymmetry of the ion pair. Secondly, the electrostatic potential minima of the nitro oxygen atoms in the *para* position are always more negative (indicating more basic atoms) by 15–30 kJ mol^{-1} than the nitro oxygen atoms in the *ortho* positions. The *para*-nitro group appears therefore as the major site of association of a hydrogen-bond donor in the ion pairs. Thirdly, as observed in Table 2 for the NZ_4^+ fragment, the geometrical parameters of the corresponding tetramethylammonium picrate ($NMe_4^+Pic^-$) model differ significantly from those of all the other substituted cations. The longer charge separation in $NMe_4^+Pic^-$ reduces the withdrawing effect of the positive charge on the electrons of the phenolate oxygen atom. Thus, the internal charge transfer of this negative oxygen atom toward the nitro groups is considerably en-

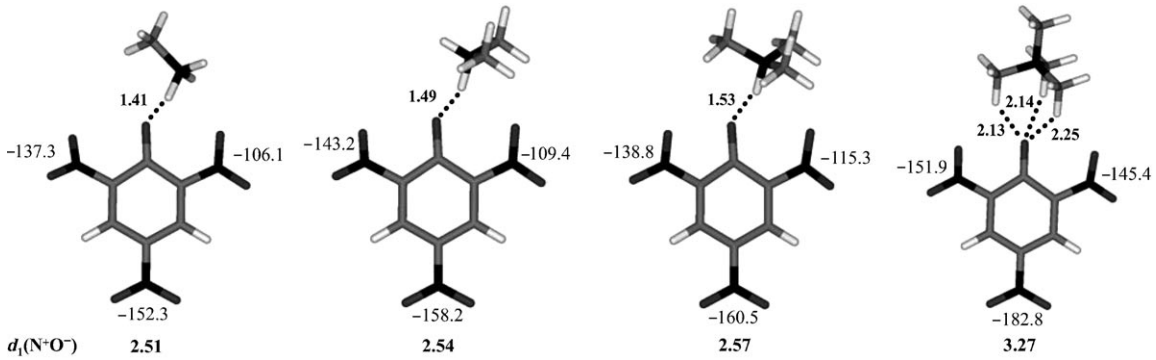

Figure 5. Geometries [Å] and local electrostatic potential minima [kJ mol^{-1}] of alkylammonium picrates (from left to right: $MeNH_3^+$, $Me_2NH_2^+$, Me_3NH^+ and NMe_4).

hanced giving much more basic nitro HB accepting sites. Finally, the distances *d* computed for the ammonium species bearing at least one hydrogen atom correspond to strong HBs, as revealed by the $(N^+)H\cdots O^-$ distances (from 1.41 to 1.53 Å). These theoretical tendencies are in good accord with the former solid-state observations. They also follow the order of measured nAChR–agonist affinities because the ligands bearing tertiary (nicotine, cytosine) or secondary ammonium moieties (epibatidine) generally have greater affinities than ACh-like ligands carrying quaternary ammoniums.[7,12]

Exploration of the NicH$^+$Pic$^-$ and AChPic$^-$ potential energy surfaces (PES): In order to scan thoroughly the potential energy surfaces (PESs) of the cation–anion interactions in NicH$^+$Pic$^-$ and AChPic$^-$ ion pairs, an intermolecular model potential was used to optimise the interaction geometry between the two ions, starting with 400 initial structures (see the Experimental Section for details). Two stable conformers, denoted **A** and **B**,[30] in which the pyridine and pyrrolidine rings are roughly perpendicular to one another, have previously been found for the naked NicH$^+$ cation. As the energy difference between these two rotamers is insignificant, two PESs were investigated: the interaction of each of the two conformers with the picrate anion. The most significant minima for the three ion pairs were then fully optimised at the B3LYP/6-31+G** level of theory.

In agreement with the trends revealed by crystallographic analysis, the phenolate oxygen atom is found again to be, in vacuo, the predominant interaction site of the picrate anion (motif A). An interaction with the *para*-nitro group (motif C) only occurs in NicH$^+$Pic$^-$ and is too unfavourable to be significant (about 65 and 80 kJ mol^{-1} above the most stable A motif, respectively, for the **A** and **B** isomers), whereas the interaction geometries of motif B do not lead to any minimum. In this system, the optimised ion pairs have very distinct energies depending on the cationic isomer. Interactions with rotamer **B** are significantly destabilised (by at least 8.6 kJ mol^{-1}) in comparison with the global minimum and so they have not been further considered in this study. In accord with the crystal data, the most stable ion pair corresponds to the one in which the phenolate oxygen atom interacts with the NH$^+$ ammonium group. Note that not less than three different orientations of the picrate anion with respect to the nicotinium cation are found within a range of 3.6 kJ mol^{-1}, corresponding to 97% of the ion-pair population in the NicH$^+$Pic$^-$ system. The AChPic$^-$ PES is in good agreement with the previous electrostatic potential analysis. Indeed, the $CH_2N^+(CH_3)_3$ tetrahedron face showing the greatest $V_{s,max}$ value is involved in the three most stable structures found. These geometries correspond to 86% of the ion-pair population in the AChPic$^-$ complexes and thus the complexes relative to the three other faces are considered negligible.

Finally, the tertiary ammonium cation gives an interaction energy 50 kJ mol^{-1} stronger than the quaternary one ($\Delta E_{el}=-364$ and -313 kJ mol^{-1}, respectively). In the same vein, optimisations of the NicH$^+$Cl$^-$ ($\Delta E_{el}=-462$ kJ mol^{-1}) and AChCl$^-$ complexes ($\Delta E_{el}=-388$ kJ mol^{-1}) indicate the stronger HB donor ability of the tertiary ammonium cation and the stronger HB acceptor ability of the chloride relative to the picrate anion.

Calibration of HF hydrogen-bond association with pyridine and ester families: Following the preliminary analysis of Lamarche and Platts,[38] we have recently shown[39] that the experimental pK_{HB} HB basicity scale of pyridine Nsp^2 and amide-ketone CO bases can be precisely predicted from the variation in the electronic energies ΔE_{el} for their association with hydrogen fluoride provided that the data for the two families are considered separately. In this study, we used Equation (1) to determine pK_{HB} values for the association of pFP with pyridine sp^2 nitrogen sites of nicotine-like cations. We also calibrated a new family corresponding to the association with oxygen esters in order to determine the basicity of the carbonyl site of ACh and its models with the best possible precision. These experimental and theoretical data are presented in Table 3 and lead to Equation (2). The validity of this latter equation can be tested with 2-dimethylaminoethyl acetate, a bifunctional Nsp^3+CO ester base. Experimentally, the only accessible constant is $K_t=63$ dm^3 mol^{-1} and this constant can be separated into the two

Table 3. Experimental and theoretical energies of HB association with esters.

Compound	Formula	Experimental donor: pFP pK_{HB}	Theoretical donor: HF $-\Delta E_{el}$ [kJ mol^{-1}]
methyl 1,1,1-trichloroacetate	CCl_3CO_2Me	0.11[a]	32.3
2,2,2-trichloroethyl acetate	$MeCO_2CH_2CCl_3$	0.47[b]	40.8
ethyl formate	HCO_2Et	0.66[a]	41.7
2-chloroethyl acetate	$MeCO_2CH_2CH_2Cl$	0.81[b]	43.2
methyl benzoate	$C_6H_5CO_2Me$	0.89[a]	44.2
methyl acetate	$MeCO_2Me$	1.00[a]	45.9
methyl 3,3-dimethylacrylate	$Me_2C{=}CHCO_2Me$	1.02[b]	45.2
2-dimethylaminoethyl acetate	$MeCO_2CH_2CH_2NMe_2$	[c]	46.7
ethyl acetate	$MeCO_2Et$	1.07[a]	47.0
propyl acetate	$MeCO_2CH_2CH_2CH_3$	1.11[b]	47.1
ethyl *trans*-dimethylaminoacrylate	$Me_2NCH{=}CHCO_2Et$	2.11[b]	61.1

[a] See ref. [40]. [b] This work. [c] Bifunctional (tertiary amine + carbonyl ester) compound: the experimental constant is $K_t = 63$ dm^3 mol^{-1}.

of 0.74 between the protonated and the neutral species corresponds to a decrease of 5 kJ mol^{-1} in Gibbs free energy. In the same way, the carbonyl group basicity of AChPic$^-$ is significantly less than that of 2-dimethylaminoethyl acetate ($\delta pK_{HB} = 0.57$). Finally, the tertiary ammonium NicH$^+$ exhibits a greater maximum electrostatic potential and higher binding energies with both picrate and chloride than the quaternary ammonium ACh. In summary, the theoretical calculations show that both charged ligands keep a significant HB basicity and that protonated nicotine appears not only slightly more basic, but also much more acidic than ACh.

individual contributions by using the frequency shifts method[41,42] as follows. In addition to its free OH band at $\tilde{\nu} = 3644$ cm^{-1}, the association of methanol with this base in CCl_4 presents two large OH absorptions at 3571 and 3276 cm^{-1} corresponding to associations with the carbonyl and tertiary amine groups, respectively. The correlation between $\Delta\tilde{\nu}$(OH) and pK_{HB} proposed by Besseau et al.[40] for the ester family allows an experimental value to be calculated: $pK_{HB} = 0.94$. On the other hand, the variation of the electronic energy of the most stable complex (Table 3) yields $pK_{HB} = 1.05$ by using Equation (2). Thus, both indirect experimental and calculated pK_{HB} values agree fairly well with the value expected for an acetate carbonyl group substituted in the γ position by a weak electron-withdrawing group.[43]

$$pK_{HB\,(\text{pyridinic sp}^2\text{ nitrogen})} = -0.1057\,\Delta E_{el} - 4.464 \quad (1)$$
$$r = 0.9995,\ n = 11,\ s = 0.03$$

$$pK_{HB\,(\text{C=O esters})} = -0.0719\,\Delta E_{el} - 2.302 \quad (2)$$
$$r = 0.991,\ n = 10,\ s = 0.07$$

Hydrogen-bonding ability of ACh and NicH$^+$: The results of the theoretical calculations on the most stable ionic forms of the two ligands are summarised in Table 4. Comparison of the minimum electrostatic potentials of the carbonyl group and the pyridine nitrogen atom indicates that 1) the strong electron-withdrawing charge of the positive nitrogen atom totally depletes the HB basicities of the acceptor sites in both naked cations (compare ACh with 2-dimethylaminoethyl acetate and NicH$^+$ with nicotine), 2) these basic sites recover proportionally greater HB affinities when their positive charges are neutralised by more basic anions ($Cl^- > Pic^-$) and 3) the $V_{s,min}$ values for the two cations in the picrate salts are still very different from those of their neutral reference bases indicating a substantial loss of basicity between the neutral models and their picrate salts. The electronic energy values ΔE_{el} confirm the notable reduction in sp^2 nitrogen HB basicity of nicotine resulting from protonation of the pyrrolidine nitrogen atom. The pK_{HB} difference

Table 4. Theoretical estimations of the HB accepting strength of ACh and nicotine cations.

Compound	$V_{s,min}$ [kJ mol^{-1}]	$-\Delta E_{el}$[a] [kJ mol^{-1}]	pK_{HB}	$V_{s,max}$ [kJ mol^{-1}]
		C=O site		N$^+$ site
ACh	+114.1			+502.6
ACh Pic$^-$	−88.6	38.7	0.48[b]	
ACh Cl$^-$	−105.8			
2-dimethylaminoethyl acetate	−152.0	46.7	1.05[b]	
		Nsp^2 site		N$^+$ site
NicH$^+$(**A**)[c]	+93.5			+593.2
NicH$^+$ Pic$^-$ (**A**)[c]	−113.5	55.2	1.37[e]	
NicH$^+$ Cl$^-$ (**A**)[c]	−132.0			
nicotine (**A**)[c]	−163.3	62.2	2.11[d]	

[a] Hydrogen-bond binding energies for the complexation with HF. [b] Calculated from Equation (2). [c] Rotamer **A** (see text). [d] Calculated from Equation (1).

Experimental determination of the basicities

HB basicity of the anion: The experimental data for the picrate derivatives of nicotine, ACh and their model amines are shown in Table 5. The frequency shifts $\Delta\tilde{\nu}_{OH}(NO_2)$ of the 4-fluorophenol (pFP) hydroxy vibration upon association with the nitro groups clearly characterise two distinct series of ammonium picrates, in line with the trends revealed by crystal and theoretical data. On the one hand, the very large $\Delta\tilde{\nu}_{OH}$ shifts of the three quaternary ammonium picrates **2**, **10** and **11** indicate the very important HB basicity of their nitro oxygen atoms.[44,45] The thermodynamic quantification of this basicity is given by the total equilibrium constant K_t of the tetrabutylammonium (**10**) and trimethyldodecylammonium (**11**) picrates in which the only potential basic sites are located on the *para*-nitro groups of the picrate anions (see above). Unexpectedly, the significant reduc-

Table 5. Association of 4-fluorophenol with ammonium picrates. Equilibrium constants and frequency shifts in dichloromethane.

Compound no.	Picrate (Pic^-)[a]	$\Delta\tilde{\nu}_{OH}(NO_2)$ [cm^{-1}][b]	K_t[c] [dm^3mol^{-1}]	K_{C^+}[d] [dm^3mol^{-1}]	K_{Pic^-}[e] [dm^3mol^{-1}]	n[f]
3	pyrrolidinium	112	5.3	–	5.3	2
4	methyldodecylammonium	120	2.7	–	2.7	4
5	*N*-methylpyrrolidinium	119	3.9	–	3.9	2
6	*N*,*N*-dimethyldodecylammonium	115	3.1	–	3.1	4
1	nicotinium ($NicH^+$)	108	14.5	9.7	(4.8)	3
7	*N*,*N*-dimethylaminomethylpyridinium (Me_2AMP)	112	12.4	8.7	(3.7)	4
8	*N*-ethyl-*N*-methylaminomethylpyridinium (Et-MeAMP)	108	10.4		(3.8)	1
9	noracetylcholine (norACh)	111	2.8			2
10	tetrabutylammonium	369	22.9[g]	–	22.9	2
11	trimethyldodecylammonium	364	23.6	–	23.6	4
2	acetylcholine (ACh)	359	22.7			9

[a] The acronyms of the compounds used throughout the text are indicated in parentheses. [b] Frequency shift of pFP upon association with the nitro group. [c] Equilibrium constant determined from the OH absorption of pFP: $K_t = K_{C^+} + K_{Pic^-}$. [d] Experimental individual association constants measured at the pyridinic site of the cation. [e] Experimental or calculated (in parentheses) equilibrium association constants measured for the picrate anion. [f] Number of independent measurements. [g] Kuntz (see ref. [20]) found $K_t = 20\ dm^3mol^{-1}$ for the phenol–tetrabutylammonium picrate complex in the same solvent.

tion in the effective size of the trimethylammonium head of **11** by comparison with the tributylammonium head of **10** does not induce any great change in nitro basicity. In the same vein, on passing from the alkylated model **11** to ACh (**2**), the presence of an electron-attracting acetoxy substituent in **2** does not influence the frequency shift $\Delta\tilde{\nu}_{OH}$ due to the association with the nitro group. On the other hand, the substitution of the first alkyl group of a quaternary ammonium cation by a hydrogen atom leads to a very large decrease in the OH frequency shift. The lower basicity of the nitro groups of the tertiary ammonium picrates **1** and **5**–**9** can be attributed to the lower tendency of the phenolic negative charge to delocalise in the picrate ring as it is held back by the hydrogen bond between the two ions.[46,47] Substitution of a second alkyl group by a hydrogen atom in the pyrrolidinium (**3**) and methyldodecylammonium (**4**) cations causes little change in basicity, as previously observed by Witschonke and Kraus.[48] One can expect a strengthening of the cation···anion hydrogen bond when an electron-withdrawing pyridinyl substituent is added to the molecule leading to a further decrease in the anion basicity. However, direct comparison of the association constants for the association of pFP on the nitro groups of *N*-methylpyrrolidinium (**5**) and *N*,*N*-dimethyldodecylammonium (**6**) picrates on the one hand and nicotinium (**1**), Me_2AMP (**7**) and EtMeAMP (**8**) picrates on the other, does not show any influence of the substituent. Thus, we can safely predict that the mean value of $K_{Pic^-} = 3.8\ dm^3mol^{-1}$ for compounds **1** and **5**–**7** also holds for EtMeAMP (**8**). This conclusion is supported by the similar frequency shifts observed for these compounds.

HB basicity of the nicotine and ACh cations: The missing equilibrium constant corresponding to the association of pFP with the accepting pyridinic nitrogen atom of the Et-MeAMP cation (**8**) can then be obtained by simple subtraction: $K_{C^+} = K_t - K_{Pic^-} = 6.6\ dm^3mol^{-1}$. The situation is different for the HB associations of pFP on the carbonyl groups of the ACh (**2**) and norACh (**9**) cations which require specific evaluations. Independent estimations of these basicities can be obtained from their carbonyl absorptions because the C=O stretching frequency is known to be a very sensitive probe of molecular interactions of carbonyl groups. The limiting condition is that mass and coupling effects are minimised by using compounds with similar structures.[49,50] We therefore completed our database on the hydrogen-bond basicity pK_{HB} (in CCl_4) of esters[40] by studying two methyl acetates substituted by electron-attracting atoms on the ether moiety in order to mimic more closely the substituent effect of the positive nitrogen atom in ACh and norACh. The pK_{HB} data reported in Table 6 can be converted into $\log K$ values in dichloromethane by using Equation (3), the linear free energy relationship (LFER) relevant to the family of carbonyl compounds studied herein. Then, the good linear relationship [Equation (4)] obtained between the thermody-

Table 6. Equilibrium constants and carbonyl frequencies for the association of pFP with some esters substituted on the ether group.

Compound	$\tilde{\nu}_{C=O}(CH_2Cl_2)$ [cm^{-1}]	$pK_{HB}(CCl_4)$	$\log K(CH_2Cl_2)$	$K(CH_2Cl_2)$ [dm^3mol^{-1}]
$MeCOOCH_2CCl_3$	1759.8	0.47	−0.15[a]	0.70
$MeCOOCH_2CH_2Cl$	1742.7	0.81	0.14[a]	1.39
$MeCOOCH_3$	1739.5	1.00[b]	0.31[a]	2.04
$MeCOOCH_2CH_3$	1733.3	1.07[b]	0.37[a]	2.36
$MeCOOCH_2CH_2NMe_2H^+$ (NorACh Pic^-; **9**)	1750.4	–	0.03[c]	1.08
$MeCOOCH_2CH_2NMe_3^+$ (ACh Pic^-; **2**)	1753.5	–	−0.03[c]	0.94

[a] Calculated from the pK_{HB} value by using Equation (3). [b] See ref. [40]. [c] Calculated from $\tilde{\nu}_{(C=O)}$ by using Equation (4).

namic parameter $\log K$ and the carbonyl frequency enables the equilibrium constants for the association of the carbonyl site with the two cations **2** and **9** to be calculated (Table 6).

$$\log K(CH_2Cl_2) = 0.878\,pK_{HB} - 0.56 \quad r = 0.997,\ n = 14,\ s = 0.05 \tag{3}$$

$$\log K(CH_2Cl_2) = -0.0205\,\tilde{\nu}_{C=O} + 35.8 \quad r = 0.984,\ n = 4,\ s = 0.05 \tag{4}$$

The comparison of the anion–cation interactions of ACh and norACh picrates through their carbonyl and nitro probes is totally coherent with previous observations. Thus, the presence of an $(N^+)H\cdots O^-$ hydrogen bond in norACh Pic^- definitely results in a neutralisation of the two opposite charges leading concomitantly 1) to an attenuation of the electron-withdrawing inductive effect of the ammonium substituent on the carbonyl group (the carbonyl group is more basic, Table 6) and 2) to a large reduction in the electron-donating resonance effect of the phenolic oxygen negative charge on the nitro group (the nitro group is less basic, Table 5).

Table 7. Hydrogen-bond basicity of the anionic and cationic sites of the ligand picrates.

Compound no.	Picrate (Pic^-)	$K(CCl_4)$	pK_{HB}	$K(CCl_4)$	pK_{HB}
		Nsp^2 cation site		NO_2 anion site	
1	Nic	27.5	1.44	40.7	1.61
7	Me_2AMP	24.4	1.39	30.7	1.49
8	EtMeAMP	18.1	1.26	31.6	1.60
		C=O cation site		NO_2 anion site	
9	norACh	4.9	0.69	13.1	1.12[a]
2	ACh	4.2	0.62	213.0	2.33[a]

[a] Obtained from the difference $K_t - K_C^+$ in CH_2Cl_2 and converted to the corresponding value in CCl_4 by using Equation (6).

Finally, we have summarised in Table 7 the individual association constants of the pFP on the pyridyl and carbonyl sites of the different ligands. These data were obtained from the results given in Tables 5 and 6 and were converted from dichloromethane to CCl_4 using the LFERs described by Equations (5), (6) and (7), which correspond, respectively, to the different families of the pyridinic sp^2 nitrogen, the nitro oxygen (among other oxygen bases) and the carbonyl oxygen bases.

$$Nsp^2: \quad pK_{HB} = 1.094 \log K(CH_2Cl_2) + 0.36 \quad r = 0.9997,\ n = 7,\ s = 0.02 \tag{5}$$

$$O(NO_2): \quad pK_{HB} = 1.092 \log K(CH_2Cl_2) + 0.87 \quad r = 0.997,\ n = 15,\ s = 0.09 \tag{6}$$

$$O(C{=}O): \quad pK_{HB} = 1.132 \log K(CH_2Cl_2) + 0.65 \quad r = 0.997,\ n = 14,\ s = 0.06 \tag{7}$$

As predicted by the theoretical calculations, the sp^2 nitrogen atom of nicotine keeps a significant basicity in the monoprotonated form since the electron-withdrawing effect of the ammonium charge is largely neutralised by the interaction with the picrate anion. Experimentally, the equilibrium constant for the association of pFP with the sp^2 nitrogen atom of nicotine picrate is seven times greater than the association constant for the interaction with the carbonyl group of ACh picrate. The corresponding ratio (corresponding to 5 kJ mol^{-1} in free energy units) measured for the cations does not differ significantly from that found in the corresponding neutral forms (K(nicotine) = 108;[51] K(2-dimethylaminoethyl acetate) = 9.9) and seems to be insensitive to the nature of the counterion, as indicated by our $V_{s,min}$ calculations on the hydrochloride salts (Table 4).

Comparison with docking energies: In the last few years, the X-ray crystal structure of AChBP has been used to build, through homology modelling, the LBD of nAChR subtypes. From these three-dimensional atomic models, molecular docking of ACh, nicotine and epibatidine into nAChR binding sites has been achieved. Through their docking studies of nicotine and ACh into homomeric chick α7 nAChR, Le Novère et al.[52] estimated a greater binding free energy (of about 6 kJ mol^{-1}) for nicotine. Similarly, Schapira et al.[53] docked both ACh and nicotine into the $\alpha4\beta2$, $\alpha3\beta2$ and $\alpha7$ atomic models. They found that the inclusion of a water molecule in the binding pocket provides additional stability to the complexes by forming small arrays of hydrogen bonds between the accepting sp^2 nitrogen atom of nicotine or the carbonyl oxygen of ACh and residues of the surrounding protein. In these studies, nicotine is again favoured by about 3 kJ mol^{-1} compared with ACh. Celie et al.[7] confirmed the presence of a bridging water molecule in high-resolution crystallographic structures of nicotine–AChBP complexes. Furthermore, their thermodynamic measurements of the ligand dissociation by isothermal titration calorimetry ($\Delta G = -34.6$ and -41.8 kJ mol^{-1} for ACh and nicotine, respectively) correctly match the docking results. Of all the interactions, the numerous HBs created between the ligands and the protein may play a crucial role. Those involving the accepting centres of the ligand have long been recognised as essential features of the nicotinic pharmacophore,[8,10] but they have never been quantified: first, because the HB donor was not known and secondly, because the acceptor atoms belong to charged molecules for which there are no reference data in the literature. Quantitative LFERs between numerous kinds of donor have been set up by Abraham and co-workers[54,55] so that, provided the pK_{HB} value of an accepting group is known, its equilibrium association constant with water can be calculated. In this analysis, equilibrium constants of $K = 2.1$ and 0.7 dm^3 mol^{-1} were obtained for the $HOH\cdots Nsp^2$ (nicotine) and $HOH\cdots O{=}C$ (ACh) complexes, respectively. The energy difference of 2.7 kJ mol^{-1} between the two associations corresponds fairly well to the differentials measured by calorimetry or calculated with the docking models. One must bear in mind that the specific hy-

drogen-bond energy between a water molecule and the accepting centre of the ligand is only one component of the total interaction energy expressed in the experimental ΔG measured by calorimetry. We have also seen that the dramatic differences in the HB donating properties of the two cationic heads play a crucial role in their interactions with the picrate anion. Owing to the number and diversity of the hydrogen bonds involved in the docking process, this result appears to be a first quantitative step in the understanding of multiple ligand interactions with nAChRs.

Experimental Section

X-ray crystallography: A crystal of nicotinium picrate was mounted on the tip of a Lindemann capillary using solvent-free glue. The intensity was measured at 150 K on a Bruker-Nonius Kappa CCD diffractometer using graphite-monochromatised Mo_K-$L_{2,3}$ radiation ($\lambda = 0.71073$ Å) and an Oxford cryostream cooler to obtain the low temperature. Data were corrected for Lorentzian polarisation effects and absorption corrections were applied using a Gaussian integration. Friedel pairs were merged. The structure was solved by Sir2004 direct methods[56] and subsequent calculations were carried out using the Jana2000 program package.[57] All non-hydrogen atoms were refined anisotropically and hydrogen atoms were introduced with geometrical constraints and riding atomic displacement parameters.

CCDC 604836 contains the supplementary crystallographic data for this paper. These data can be obtained free of charge from the Cambridge Crystallographic Data Centre via www.ccdc.cam.ac.uk/data_request/cif.

Crystal data for nicotinium picrate: $C_{16}H_{17}N_5O_7$; $M_r = 391.3$; orthorhombic; $P2_12_12_1$; $a = 7.2166(4)$, $b = 12.4243(6)$, $c = 19.5563(16)$ Å; $V = 1753.44(19)$ Å^3; $Z = 4$; $\rho_{calcd} = 1.4819$ g cm^{-3}; $\mu = 0.119$ mm^{-1}; $F(000) = 816$; yellow plate; $0.5 \times 0.4 \times 0.13$ mm^3; $2\theta_{max} = 69.98°$; $T = 150$ K; 21072 reflections, 4277 unique (99% completeness); $R_{int} = 0.075$; 253 parameters; GOF = 2.26; $wR_2 = 0.1212$; $R = 0.0449$ for 2604 reflections with $I > 2\sigma(I)$.

Cambridge structural database searches: Crystallographic data were retrieved from the 5.27 release (November 2005, 355064 entries) of the CSD.[58] The ConQuest program[59] was used to search for bonded substructures and intermolecular non-bonded contacts. The structures were visualised with MERCURY[59] and the geometrical data analysis was performed with VISTA.

Among the 384 entries containing the picrate fragment, we found 157 crystal structures with an ammonium group. We then arranged the ammonium substructures according to the degree of nitrogen substitution. At this stage, we looked for $N^+\cdots O^-$ contacts as a function of the picrate site of association and the degree of ammonium nitrogen substitution. In the first step of this work, an intermolecular contact was defined as in the IsoStar library,[24] that is, as any contact shorter than $V + 0.5$ Å, where V is the sum of the Bondi van der Waals radii. In the present case, this criterion corresponds to a distance of 3.6 Å.[25] In a second step this criterion was reduced to V (3.1 Å) in order to investigate the shortest contacts.

Theoretical calculations: All calculations were performed at the B3LYP/6-31+G** level of theory using the Gaussian 03[60] package supported on the CCIPL, CINES and IDRIS supercomputers.

The starting geometries for the ion pairs must take into account not only the conformational flexibility of the cation, but also the relative positions of the anion and cation. Starting from the fully optimised monomer structures (B3LYP/6-31+G**), the PES of the ion-pair interaction can be thoroughly scanned in the rigid-body approximation using an intermolecular model potential based on an accurate distributed multipole analysis (DMA) for the dominant electrostatic term. The interaction geometry was optimised starting from 400 points randomly generated at both short and long distances. This approach led to a limited number of complexes which were then fully optimised at the B3LYP/6-31+G** level of theory. The model potential, dubbed MP2fit/DMA, has been fully described previously.[15,61–63] It consists of an atom–atom 6-exp potential to depict the repulsion and dispersion terms augmented with an accurate distributed multipole analysis (DMA)[64,65] model to depict the dominant electrostatic interaction term. The GDMA[66] program was used to compute the DMA models from the Gaussian MP2/6-311G**//B3LYP/6-31+G** monomer wave functions and the model potential of the ion pairs was calculated with the ORIENT program.[67]

Electrostatic potentials around all the optimised ion pairs were mapped on the 0.001 electron bohr^{-3} contour of the electronic density.

The HB ability of the basic sites (the pyridine sp^2 nitrogen or the carbonyl oxygen atom in the reference compounds and in the salts) was calculated in vacuo using hydrogen fluoride (HF) as the HB donor probe [Equation (8)]). HF has already been used with success to predict HB energetic parameters both for charged[16] and neutral[39] forms of ligands through LFERs between the experimental Gibbs energy of pFP complexation, ΔG°_{298} (ΔG°_{298}/kJ mol^{-1} $= -5.71 pK_{HB}$), measured in CCl_4, and the calculated density functional (B3LYP/6-31+G**) electronic energy variation ΔE_{el} of HF complexation. In this work, the binding energy of HF to a basic site was calculated through Equation (9) according to the supermolecule approach.

$$\text{Base} + \text{HF} \rightleftharpoons \text{Base}\cdots\text{HF} \tag{8}$$

$$\Delta E_{el} = E_{el}(\text{Base}\cdots\text{HF}) - E_{el}(\text{HF}) - E_{el}(\text{Base}) \tag{9}$$

The basis set superposition error (BSSE) was not taken into account because it is expected to be quasiconstant within the two homogeneous families of pyridines and carbonyl model compounds that are considered separately in this study. All stationary points (molecular bases, ion pairs and their HB complexes) were confirmed as true minima by vibrational frequency calculations.

Synthesis and purification: 2,2,2-Trichloroethyl acetate and 2-choroethyl acetate were synthesised by standard methods from the corresponding alcohol and acetic anhydride in the presence of pyridine. The compounds were distilled, dried over molecular sieves and their purity checked by gas-phase chromatography. The picrates were generally synthesised by direct reaction of the amine with picric acid in methanol/water or ethanol/water. Quaternary ammonium picrates were obtained by precipitation of silver iodide between silver picrate and the ammonium iodide.[17] The crystals were recrystallised in ethanol/water and carefully dried under vacuum. Their purity was checked by thin-layer chromatography and infrared spectroscopy.

FTIR spectroscopy: The experimental determination of the strength of a remote hydrogen-bond accepting site in an organic cation, such as the pyridinic nitrogen of the nicotinium ion (**1**) or the carbonyl oxygen of ACh **2**, is drastically affected by the nature of the counteranion A^-.

The association equilibrium constants of a reference donor 4-fluorophenol (pFP) on the C^+Pic^- salts and on some neutral carbonyl bases were measured by FTIR spectroscopy using the model system selected to define the general HB basicity scale pK_{HB}[68,69] [Equations (10) and (11)].

$$4\text{-}FC_6H_4OH + C^+Pic^- \rightleftharpoons 4\text{-}FC_6H_4OH\cdots C^+Pic^- \tag{10}$$

$$K_c(25\,^\circ\text{C}) = \frac{[4\text{-}FC_6H_4OH\cdots C^+Pic^-]}{[C^+Pic^-][4\text{-}FC_6H_4OH]} \tag{11}$$

The concentrations $[4\text{-}FC_6H_4OH\cdots C^+Pic^-]$, $[C^+Pic^-]$ and $[4\text{-}FC_6H_4OH]$ in Equation (11) were calculated from the equilibrium infrared absorption intensities and from the weighted initial amounts of the donor and acceptor. For the picrate salts, which are sparingly soluble in carbon tetrachloride, all measurements were carried out in dichloromethane and the experimental data converted to the reference pK_{HB} scale (in CCl_4) using calibrated family-dependent LFERs.[16] Owing to the very low transparency of dichloromethane in the OH region and to the low solubility of some salts, the precision of the equilibrium constants, carried out in 10, 2 and 1 mm quartz or fluorine cells, is estimated to be about 15–20%. The frequency shifts are accurate to 5–10 cm^{-1}.

The decrease in the OH absorption of the donor induced by the introduction of the salt into solution is a consequence of the association of pFP with all the available accepting sites. Therefore, the calculated equilibrium constant K_t is the sum of the individual 1:1 equilibrium constants[39] for the C^+ cation and Pic^- anion [Equations (12)–(14)].

$$4\text{-}FC_6H_4OH + C^+Pic^- \rightleftharpoons 4\text{-}FC_6H_4OH \cdots C^+Pic^- \qquad K_{C^+} \qquad (12)$$

$$4\text{-}FC_6H_4OH + C^+Pic^- \rightleftharpoons 4\text{-}FC_6H_4OH \cdots Pic^-C^+ \qquad K_{Pic^-} \qquad (13)$$

$$K_t = \frac{[4\text{-}FC_6H_4OH \cdots C^+Pic^-] + [4\text{-}FC_6H_4OH \cdots Pic^-C^+]}{[4\text{-}FC_6H_4OH][C^+Pic^-]} = K_{C^+} + K_{Pic^-} \qquad (14)$$

In a few favourable systems in which dibasic species show intense characteristic absorptions shifted by association, the two individual equilibrium constants can be obtained from additional infrared experiments.[39] For instance, the individual association constant for the Nsp^2 site of the nicotinium cation **1** has been obtained separately from the pyridine $\tilde{\nu}_1$ vibration at 1026 cm^{-1}.[16] In most cases, however, the only direct quantitative information is the total equilibrium constant. Various indirect methods for their separation into individual association constants have been used that involve 1) experimental $\Delta\tilde{\nu}$(OH) frequency shifts,[41,42] 2) substituent effects,[51,70] 3) molecular fragment models[71] or 4) theoretical descriptors.[42,72,73]

Acknowledgements

The authors gratefully acknowledge Aurélien Planchat for his active participation in the experimental work, Prof. Anthony J. Stone for providing the Orient program and the Centre de Calcul Intensif des Pays de la Loire (CCIPL), the Centre Informatique National de l'Enseignement Supérieur (CINES) and the Institut Des Ressources en Informatique Scientifique (IDRIS) for computer time.

[1] J. A. Dani, M. De Biasi, Y. Liang, J. Peterson, L. Zhang, T. Zhang, F. M. Zhou, *Bioorg. Med. Chem. Lett.* **2004**, *14*, 1837–1839.
[2] P. Newhouse, A. Singh, A. Potter, *Curr. Top. Med. Chem.* **2004**, *4*, 267–282.
[3] R. C. Hogg, M. Raggenbass, D. Bertrand, *Rev. Physiol. Biochem. Pharmacol.* **2003**, *147*, 1–46.
[4] T. Grutter, J. P. Changeux, *Trends Biochem. Sci.* **2001**, *26*, 459–463.
[5] A. Miyazawa, Y. Fujiyoshi, N. Unwin, *Nature* **2003**, *423*, 949–955.
[6] K. Brejc, W. J. van Dijk, R. V. Klaassen, M. Schuurmans, J. van der Oost, A. B. Smit, L. K. Sixma, *Nature* **2001**, *411*, 269–276.
[7] P. H. N. Celie, S. E. Van Rossum-Fikkert, W. J. Van Dijk, K. Brejc, A. B. Smit, T. K. Sixma, *Neuron* **2004**, *41*, 907–914.
[8] W. H. Beers, E. Reich, *Nature* **1970**, *228*, 917–922.
[9] R. A. Glennon, M. Dukat, *Pharm. Acta Helv.* **2000**, *74*, 103–114.
[10] R. A. Glennon, M. Dukat, L. Liao, *Curr. Top. Med. Chem.* **2004**, *4*, 631–644.
[11] J. E. Tonder, P. H. Olesen, J. B. Hansen, M. Begtrup, I. Pettersson, *J. Comput. Aided Mol. Des.* **2001**, *15*, 247–258.
[12] A. L. Cashin, E. J. Petersson, H. A. Lester, D. A. Dougherty, *J. Am. Chem. Soc.* **2005**, *127*, 350–356.
[13] X. Huang, F. Zheng, P. A. Crooks, L. P. Dwoskin, C.-G. Zhan, *J. Am. Chem. Soc.* **2005**, *127*, 14401–14414.
[14] J. Graton, M. Berthelot, J. F. Gal, C. Laurence, J. Lebreton, J. Y. Le Questel, P. C. Maria, R. Robins, *J. Org. Chem.* **2003**, *68*, 8208–8221.
[15] J. Graton, T. Van Mourik, S. L. Price, *J. Am. Chem. Soc.* **2003**, *125*, 5988–5997.
[16] V. Arnaud, M. Berthelot, J.-Y. Le Questel, *J. Phys. Chem. A* **2005**, *109*, 3767–3770.
[17] S. Roelens, R. Torriti, *J. Am. Chem. Soc.* **1998**, *120*, 12443–12452.
[18] D. T. Copenhafer, C. A. Kraus, *J. Am. Chem. Soc.* **1951**, *73*, 4557–4561.
[19] K. Sawada, E. Takahashi, T. Horie, K. Satoh, *Monatsh. Chem.* **2001**, *132*, 1439–1450.
[20] I. D. Kuntz, Jr., R. P. Taylor, *J. Phys. Chem.* **1970**, *74*, 4573–4577.
[21] F. H. Allen, C. A. Baalham, J. P. M. Lommerse, P. R. Raithby, E. Sparr, *Acta Crystallogr., Sect. B* **1997**, *53*, 1017–1024.
[22] J. Harrowfield, *J. Chem. Soc., Dalton Trans.* **1996**, 3165–3171.
[23] A. Szumna, J. Jurczak, Z. Urbanczyk-Lipkowska, *J. Mol. Struct.* **2000**, *526*, 165–175.
[24] I. J. Bruno, J. C. Cole, J. P. M. Lommerse, R. S. Rowland, R. Taylor, M. L. Verdonk, *J. Comput. Aided Mol. Des.* **1997**, *11*, 525–537.
[25] A. Bondi, *J. Phys. Chem.* **1964**, *68*, 441–451.
[26] M. Evain, F. X. Felpin, C. Laurence, J. Lebreton, J. Y. Le Questel, *Z. Kristallogr.* **2003**, *218*, 753–760.
[27] T. P. Pitner, W. B. Edwards III, R. L. Bassfield, J. F. Whidby, *J. Am. Chem. Soc.* **1978**, *100*, 246–251.
[28] J. F. Whidby, J. I. Seeman, *J. Org. Chem.* **1976**, *41*, 1585–1590.
[29] T. Takeshima, R. Fukumoto, T. Egawa, S. Konaka, *J. Phys. Chem. A* **2002**, *106*, 8734–8740.
[30] D. E. Elmore, D. A. Dougherty, *J. Org. Chem.* **2000**, *65*, 742–747.
[31] J. Graton, M. Berthelot, J.-F. Gal, S. Girard, C. Laurence, J. Lebreton, J.-Y. Le Questel, P.-C. Maria, P. Naus, *J. Am. Chem. Soc.* **2002**, *124*, 10552–10562.
[32] R. B. Barlow, O. Johnson, *Br. J. Pharmacol.* **1989**, *98*, 799–808.
[33] K. Frydenvang, L. Gronborg, B. Jensen, *Acta Crystallogr. Sect. B* **1988**, *44*, 841–845.
[34] R. S. Rowland, R. Taylor, *J. Phys. Chem.* **1996**, *100*, 7384–7391.
[35] K. Sawada, F. Chigira, K. Satoh, T. Komatsuzaki, *J. Chem. Soc., Faraday Trans.* **1997**, *93*, 1903–1908.
[36] L. Troxler, J. M. Harrowfield, G. Wipff, *J. Phys. Chem. A* **1998**, *102*, 6821–6830.
[37] C. E. Cannizzaro, K. N. Houk, *J. Am. Chem. Soc.* **2002**, *124*, 7163–7169.
[38] O. Lamarche, J. A. Platts, *Chem. Eur. J.* **2002**, *8*, 457–466.
[39] V. Arnaud, J.-Y. Le Questel, M. Mathé-Allainmat, J. Lebreton, M. Berthelot, *J. Phys. Chem. A* **2004**, *108*, 10740–10748.
[40] F. Besseau, C. Laurence, M. Berthelot, *J. Chem. Soc., Perkin Trans. 2* **1994**, 485–489.
[41] M. Berthelot, C. Laurence, M. Safar, F. Besseau, *J. Chem. Soc. Perkin Trans. 2* **1998**, 283–290.
[42] E. Marquis, J. Graton, M. Berthelot, A. Planchat, C. Laurence, *Can. J. Chem.* **2004**, *82*, 1413–1422.
[43] C. Hansch, A. Leo, R. W. Taft, *Chem. Rev.* **1991**, *91*, 165–195.
[44] C. Laurence, M. Berthelot, M. Lucon, D. G. Morris, *J. Chem. Soc., Perkin Trans. 2* **1994**, 491–493.
[45] A. Chardin, C. Laurence, M. Berthelot, D. G. Morris, *Bull. Soc. Chim. Fr.* **1996**, *133*, 389–393.
[46] S. C. Mohr, W. D. Wilk, G. M. Barrow, *J. Am. Chem. Soc.* **1965**, *87*, 3048–3052.
[47] H. W. Aitken, W. R. Gilkerson, *J. Am. Chem. Soc.* **1973**, *95*, 8551–8559.
[48] C. R. Witschonke, C. A. Kraus, *J. Am. Chem. Soc.* **1947**, *69*, 2472–2481.
[49] L. J. Bellamy, *The Infrared Spectra of Complex Molecules, Vol. 2*, Chapman and Hall, London, **1980**.
[50] T. Gramstad, W. J. Fuglevik, *Acta Chem. Scand.* **1962**, *16*, 1369–1377.
[51] J. Graton, M. Berthelot, J.-F. Gal, C. Laurence, J. Lebreton, J.-Y. Le Questel, P.-C. Maria, R. Robins, *J. Org. Chem.* **2003**, *68*, 8208–8221.
[52] N. Le Novère, T. Grutter, J.-P. Changeux, *Proc. Natl. Acad. Sci. U.S.A.* **2002**, *99*, 3210–3215.
[53] M. Schapira, R. Abagyan, M. Totrov, *BMC Struct. Biol.* **2002**, *2*, 1–8.
[54] M. H. Abraham, P. L. Grellier, D. V. Prior, R. W. Taft, J. J. Morris, P. J. Taylor, C. Laurence, M. Berthelot, R. M. Doherty, M. J. Kamlet, J.-L. M. Abboud, K. Sraidi, G. Guihéneuf, *J. Am. Chem. Soc.* **1988**, *110*, 8534–8536.
[55] M. H. Abraham, P. L. Grellier, D. V. Prior, P. P. Duce, J. J. Morris, P. J. Taylor, *J. Chem. Soc., Perkin Trans. 2* **1989**, 699–711.

[56] M. C. Burla, R. Caliandro, M. Camalli, B. Carrozzini, G. L. Cascarano, L. De Caro, C. Giacovazzo, G. Polidori, R. Spagna, *J. Appl. Crystallogr.* **2005**, *38*, 381–388.
[57] JANA2000, Structure Determination Software Programs, V. Petricek, M. Dusek, Praha (Czech Republic), **2000**.
[58] F. H. Allen, R. Taylor, *Chem. Soc. Rev.* **2004**, *33*, 463–475.
[59] I. J. Bruno, J. C. Cole, P. R. Edgington, M. Kessler, C. F. Macrae, P. McCabe, J. Pearson, R. Taylor, *Acta Crystallogr. Sect. B* **2002**, *58*, 389–397.
[60] Gaussian 03, Revision C.02, M. J. Frisch, G. W. Trucks, H. B. Schlegel, G. E. Scuseria, M. A. Robb, J. R. Cheeseman, J. A. Montgomery, Jr., T. Vreven, K. N. Kudin, J. C. Burant, J. M. Millam, S. S. Iyengar, J. Tomasi, V. Barone, B. Mennucci, M. Cossi, G. Scalmani, N. Rega, G. A. Petersson, H. Nakatsuji, M. Hada, M. Ehara, K. Toyota, R. Fukuda, J. Hasegawa, M. Ishida, T. Nakajima, Y. Honda, O. Kitao, H. Nakai, M. Klene, X. Li, J. E. Knox, H. P. Hratchian, J. B. Cross, V. Bakken, C. Adamo, J. Jaramillo, R. Gomperts, R. E. Stratmann, O. Yazyev, A. J. Austin, R. Cammi, C. Pomelli, J. W. Ochterski, P. Y. Ayala, K. Morokuma, G. A. Voth, P. Salvador, J. J. Dannenberg, V. G. Zakrzewski, S. Dapprich, A. D. Daniels, M. C. Strain, O. Farkas, D. K. Malick, A. D. Rabuck, K. Raghavachari, J. B. Foresman, J. V. Ortiz, Q. Cui, A. G. Baboul, S. Clifford, J. Cioslowski, B. B. Stefanov, G. Liu, A. Liashenko, P. Piskorz, I. Komaromi, R. L. Martin, D. J. Fox, T. Keith, M. A. Al-Laham, C. Y. Peng, A. Nanayakkara, M. Challacombe, P. M. W. Gill, B. Johnson, W. Chen, M. W. Wong, C. Gonzalez, J. A. Pople, Gaussian, Inc., Wallingford CT, **2004**.
[61] T. van Mourik, S. L. Price, D. C. Clary, *Faraday Discuss.* **2001**, *118*, 95–108.
[62] T. van Mourik, *Phys. Chem. Chem. Phys.* **2001**, *3*, 2886–2892.
[63] T. van Mourik, *Phys. Chem. Chem. Phys.* **2004**, *6*, 2827–2837.
[64] A. J. Stone, *Chem. Phys. Lett.* **1981**, *83*, 233–239.
[65] A. J. Stone, M. Alderton, *Mol. Phys.* **1985**, *56*, 1047–1064.
[66] GDMA: a program for performing distributed multipole analysis of wave functions calculated using the Gaussian program system, version 1.0, A. J. Stone, University of Cambridge, Cambridge (UK), **1999**.
[67] ORIENT, version 4.4, A. J. Stone, A. Dullweber, O. Engkvist, E. Fraschini, M. P. Hodges, A. W. Meredith, P. L. A. Popelier, D. J. Wales, University of Cambridge, Cambridge (UK), **2001**.
[68] R. W. Taft, D. Gurka, L. Joris, P. von R. Schleyer, J. W. Rakshys, *J. Am. Chem. Soc.* **1969**, *91*, 4801–4808.
[69] C. Laurence, M. Berthelot, *Perspect. Drug Discovery Des.* **2000**, *18*, 39–60.
[70] F. Besseau, M. Lucon, C. Laurence, M. Berthelot, *J. Chem. Soc., Perkin Trans. 2* **1998**, 101–108.
[71] J.-Y. Le Questel, G. Boquet, M. Berthelot, C. Laurence, *J. Phys. Chem. B* **2000**, *104*, 11816–11823.
[72] J.-Y. Le Questel, M. Berthelot, C. Laurence, *J. Phys. Org. Chem.* **2000**, *13*, 347–358.
[73] C. Ouvrard, M. Lucon, J. Graton, M. Berthelot, C. Laurence, *J. Phys. Org. Chem.* **2004**, *17*, 56–64.

Received: June 9, 2006
Published online: November 14, 2006

